IMPERIAL

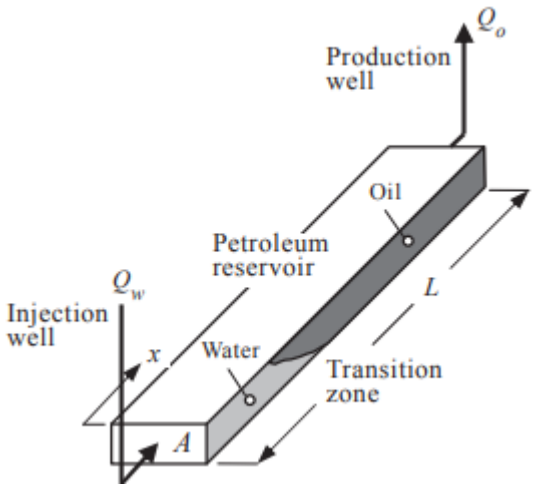

Buckley-Leverett and Spontaneous Imbibition

Coding Assessment

ABSTRACT

This study examines three different fluid displacement scenarios in porous media, focusing on how wetting and non-wetting phases interact. There is three different cases for this assessment, there are: Case 1 (CO2 – Water), Case 2 (Water – H2), and Case 3 (Water – CO2). Python code is used to calculate the analytical and numerical solution for both of Buckley Leverett and Spontaneous Imbibition. For the Buckley Leverett, we need to find the shocks in the analytical solution. And for Spontaneous Imbibition, we need to calculate the omega. Case 1 (CO_2 displacing water) is a drainage process where CO_2, being the non-wetting phase, flows more easily through larger pores. In Case 2 (Water displacing H_2), water—acting as the wetting phase—spreads into smaller pores and traps H_2 in the larger ones. And Case 3 (Water displacing CO_2) is similar to Case 2, water moves into smaller pores while trapping CO_2 in larger spaces. In summary, the study underscores the importance of capillary forces and wetting characteristics in fluid movement through porous media, with numerical simulations closely matching theoretical expectations. The numerical solutions for Cases 2 and 3 highlighting the inherent limitations due to discretization and boundary condition handling.

Zahrotuts Tsaniyah (CID: 06031044)

MSc Geo-Energy with Machine Learning and Data Science (GEMS)

1. INTRODUCTION

The Buckley-Leverett frontal displacement theory provides a method for determining saturation profiles while disregarding capillary pressure and gravity effects. Despite these simplifications, the theory became widely adopted in petroleum engineering due to its accuracy and ease of application. Early numerical approaches included the Simultaneous Solution (SS) method and the Implicit Pressure-Explicit Saturation (IMPES) method, both utilizing the Finite Difference Method (FDM). The analysis was later expanded to account for gravity, capillary pressure, fluid compressibility, and aquifer compressibility. Numerical studies using FDM revealed that, over time, saturation evolves into a multi-valued function of the grid spacing (Arabzai and Honma, 2013).

Spontaneous imbibition refers to the movement of a wetting fluid into a porous material due to capillary forces (Morrow and Mason, 2001). This process takes place only when the wetting fluid replaces the non-wetting fluid within the pore space. It typically occurs when the pore space is predominantly filled with the non-wetting fluid, requiring a positive capillary pressure difference (Anderson, 1986). Initially, the wetting fluid quickly penetrates the more permeable areas, such as fractures, before gradually being absorbed into the matrix, where the majority of the oil is stored (Al-Hadhrami and Blunt, 2001).

2. METHODOLOGY

- Parameters for Each Case

Table 1. Parameters for each case

Case/Property	Case 1	Case 2	Case 3
Phase 1	CO_2	Water	Water
Phase 2	Water	Hydrogen	CO_2
μ_1	0.1 mPa.s	1 mPa.s	0.4 mPa.s
μ_2	1 mPa.s	0.1 mPa.s	0.1 mPa.s
k_{r1}^{max}	1	0.15	0.4
k_{r2}^{max}	1	1	0.8
a	1.2	4	8
b	3	1.5	3
S_{1i}	0	0.2	0.2
S_{2r}	0.2	0.5	0.15
K	Not needed	10^{-13} m^2	10^{-13} m^2
ϕ	Not needed	0.25	0.25
P_c^{max}	Not needed	100 kPa	100 kPa
c	Not needed	0.3	0.3
S_1^*	Not needed	0.5	0.5

- The equation for relative permeability and capillary pressure:

Table 2. The equation for relative permeability and capillary pressure

Effective Saturation (Se)	Relative Permeability (kr)	Capillary Pressure (Pc)
$= \dfrac{(S_1 - S_{1i})}{(1 - S_{2r} - S_{1i})}$	➢ $k_{r1} = k_{r1}^{max} {S_e}^a$ ➢ $k_{r2} = k_{r2}^{max}(1 - S_e)^b$	$= P_2 - P_1$ $= P_c^{max} \dfrac{\left(\frac{S_1^*}{S_{1i}}\right)^{-c} - \left(\frac{S_1}{S_{1i}}\right)^{-c}}{\left(\frac{S_1^*}{S_{1i}}\right)^{-c} - 1}$

A. Buckley-Leverett

- **Analytical Solution:**

$$f_1' = \left.\frac{df_1}{ds_1}\right|_{S_v} = \frac{f_1(S_v + \Delta S_1) - f_1(S_v - \Delta S_1)}{2\Delta S_1}$$

1. Calculate the effective saturation and relative permeability using the equation from the table above.
2. Calculate the fractional flow and the derivative of this function

- Fractional flow:

$$f_1 = \frac{1}{1 + \frac{\mu_1}{\mu_2}\frac{k_{r2}}{k_{r1}}}$$

3. Calculate the dimensionless wavespeed (vD)

$$vD = \frac{\Delta f_w}{\Delta S_w}$$

4. Determine the shock and shock front saturation
   - Shock:

$$y = \frac{f_1(S_v)}{S_v - S_{1i}}$$

   - Shock front saturation:

$$tangent\ shock = 1/1 - S_{1i} - S_{2r}$$

- **Numerical Solution:**

$$\frac{\partial S_1}{\partial t_D} + \frac{\partial f_1}{\partial x_D} = 0$$

1. Define the other parameters: grid block size, time step size, number of spatial grid blocks, number of timesteps
2. Create the initialization of initial condition
3. Create time loop and spatial loop
4. Calculate the dimensionless velocity (vD)

$$v_D = \frac{x_D}{t_D} = \frac{\left(i - \frac{1}{2}\right)\Delta x_D}{n^{max}\Delta t_D}$$

B. Spontaneous Imbibition

$$\emptyset\frac{\partial S_1}{\partial t} = \frac{\partial}{\partial x}D(S_r)\frac{\partial S_1}{\partial x}$$

- **Analytical**

1. Calculate the effective saturation, relative permeability, and capillary pressure using the equation in the table above
2. Calculate the capillary dispersion and interpolate for integration

$$D = -\frac{\frac{k_{r1}}{\mu_1}\frac{k_{r2}}{\mu_2}}{\frac{k_{r1}}{\mu_1} + \frac{k_{r2}}{\mu_2}} K \frac{dP_c}{dS_1}$$

3. Calculate the C^2 using the initial guess
   - Initial guess:

$$F(S_1) = \frac{S_1 - S_{1i}}{S_1^* - S_{1i}}$$

   - C^2 function:

$$C^2 = \frac{\emptyset}{2}\int_{S_{1i}}^{S_1^*} \frac{(\beta - S_{1c})D(\beta)}{F(\beta)}\, d\beta$$

4. Find an imbibition fractional flow F1(S1)

$$F_1(S_1) = 1 - \frac{\emptyset}{2C^2}\int_{S_1}^{S_1^*}\frac{(\beta - S_1)D(\beta)}{F(\beta)}d\beta$$

5. Iterate to find F1 and C^2 values
6. Calculate the omega

$$\omega = \left(\frac{2C}{\emptyset}\right)\frac{dF}{dS_1}$$

- **Numerical**

1. Define other parameters: boundary condition at j-1, boundary condition at 2r, initial condition for all j at t=0, number of time steps, number of space steps, total space, and total time
2. Calculate the diffusion coefficient for a given saturation
3. Initialize the saturation array with the initial condition
4. Apply initial boundary condition

S1(x,t)= S1i for t=0, x>0 and S1(x,t)= S1* for t>0, x=0 where Pc(S1*)=0

5. Apply the finite difference for diffusion
6. Calculate the omega

3. RESULTS AND DISCUSSION

a. Buckley Leverett:

The analytical solution is based on the Buckley-Leverett theory, which describes two-phase flow in porous media. Just likes what I have written on the methodology above, the key steps for analytical solution include: calculate the effective saturation, relative permeability, fractional flow, dimensionless wavespeed, and the shock. I used this equation to find the shock:

$$y = \frac{f_1(S_v)}{S_v - S_{1i}}$$

The code for numerical solution here uses a finite difference method (FDM). The key numerical scheme used in this code is a first-order explicit upwind finite difference scheme to solve the Buckley-Leverett equation. Uses forward time stepping with simple updates at each grid point.

Table 3. Grid block size, time step size, and number of timesteps for each case in numerical solution of Buckley Leverett

Case	Grid Block Size	Time Step Size	Number of Timesteps
Case 1 (CO2 – Water)	0.01	0.001	200
Case 2 (Water – H2)	0.01	0.001	300
Case 3 (Water – CO2)	0.01	0.001	300

- **Case 1:**

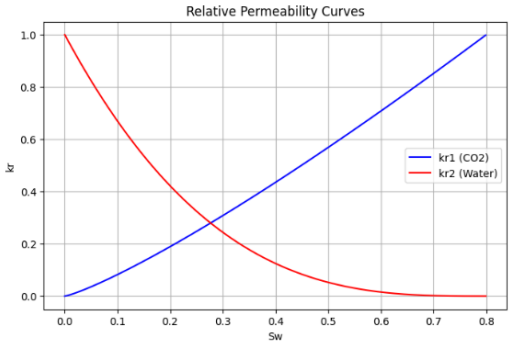

Figure 1. Relative permeability curves for Case 1

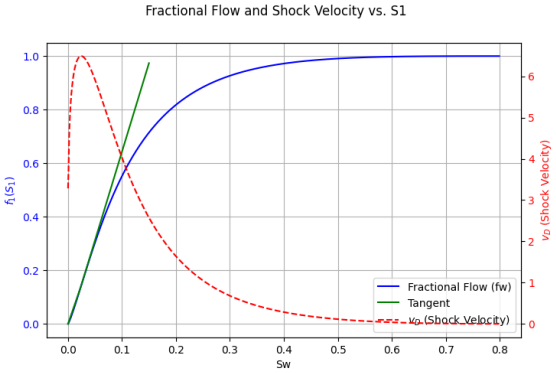

Figure 2. Fractional flow and shock velocity vs Sw for Case 1

For Case 1: The relative permeability curves (top-left plot) indicate that CO_2 (the non-wetting phase) has a higher relative permeability than water (the wetting phase) at intermediate saturations. This implies that CO_2 moves more easily through larger pores, whereas water remains trapped in smaller pores due to capillary forces.

The fractional flow function (top-right plot, blue curve) describes the proportion of CO_2 flow relative to the total fluid. The tangent construction (green line) determines the shock saturation, marking a sudden change in saturation. The steep increase in fractional flow signifies a rapidly advancing front, creating a sharp transition between CO_2 and water rather than a gradual mixing. Physically, this represents an abrupt displacement front where CO_2 forcefully pushes water out, causing water bypassing in certain areas.

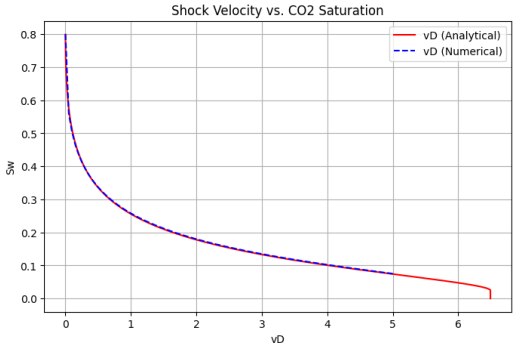

Figure 3. Comparison of numerical and analytical solution of Buckley Leverett for case 1

The numerical solution closely aligns with the analytical curve, validating the finite difference method. When shock velocity is high, saturation remains low, allowing CO_2 to penetrate the medium more quickly. As velocity decreases, the shock front slows, leading to higher saturation and greater CO_2 invasion into the reservoir.

In this scenario (CO_2 displacing water), CO_2, as the non-wetting phase, displaces water, which remains trapped in smaller pores due to capillary effects. This explains why imbibition is not applicable—imbibition occurs when the wetting phase (water) re-enters the rock, not when it is being displaced. Since Case 1 represents a drainage process, imbibition cannot be used here.

- **Case 2:**

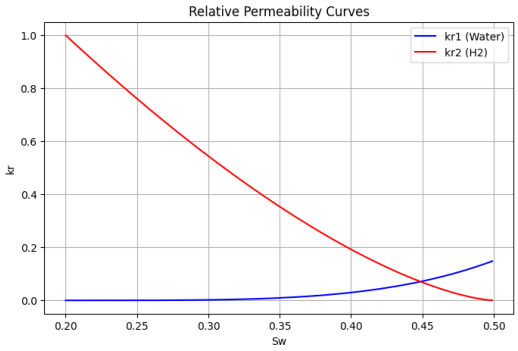

Figure 4. Relative permeability curves for Case 2

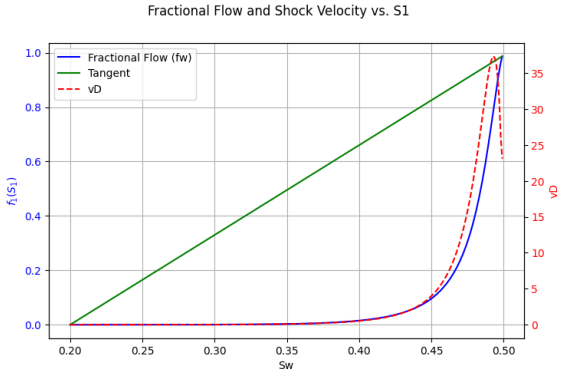

Figure 5. Fractional flow and shock velocity vs Sw for Case 2

For Case 2: The top-left plot presents two curves, one for the wetting phase (water) and another for the non-wetting phase (H_2). Since H_2 is non-wetting, its relative permeability declines rapidly as water saturation increases. This indicates that at higher water saturations, H_2 struggles to flow and can become trapped in the pore spaces. In contrast, water, as the wetting phase, maintains a higher effective permeability, allowing it to move more easily through the rock as saturation rises. Water readily channels through the pores, while H_2 encounters fewer conductive pathways, leading to significant trapping of the non-wetting phase.

The top-right plot (Fractional Flow vs. Saturation and Shock Velocity) illustrates how water's proportion of the total flow changes with saturation and how quickly the saturation front moves. The fractional flow function increases gradually at low saturations but becomes steeper as water saturation rises. Physically, this means that once the pores are filled with water, nearly all flow is carried by water. Since water retains considerable relative permeability even as H_2 saturation declines, the water front (shock) progresses steadily, displacing H_2. Once water saturation surpasses a certain threshold, the non-wetting phase becomes largely immobile, effectively "locking in" the shock front.

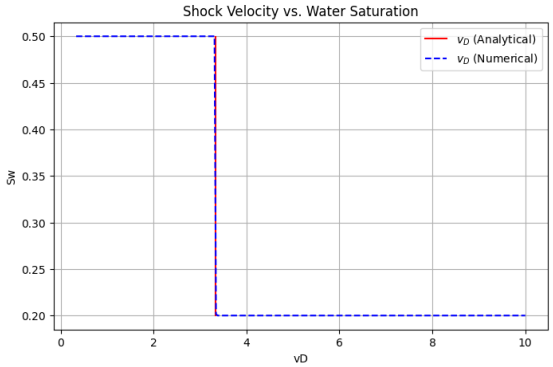

Figure 6. Comparison of numerical and analytical solution of Buckley Leverett for case 2

The numerical solution closely aligns with the analytical curve, confirming the finite difference method's accuracy. When the shock velocity is high, water saturation remains low—indicating that water (the wetting phase) is advancing quickly but with limited pore-space invasion. As velocity decreases, the shock front slows, allowing more water to occupy the pores and thus increasing the overall water saturation.

In this setup, water displaces H_2, which is the non-wetting phase. Because water is the wetting fluid, it more easily invades smaller pores, trapping H_2 in larger channels or behind the advancing

front. This behaviour reflects imbibition (wetting fluid entering a medium initially filled with non-wetting fluid), rather than drainage.

- **Case 3:**

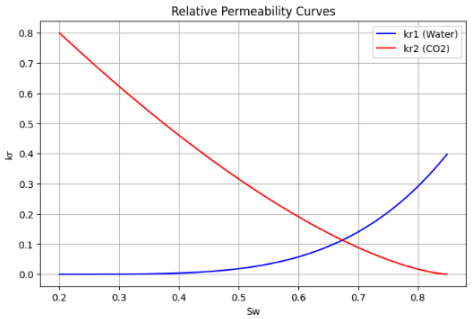

Figure 7. Relative permeability curves for Case 3

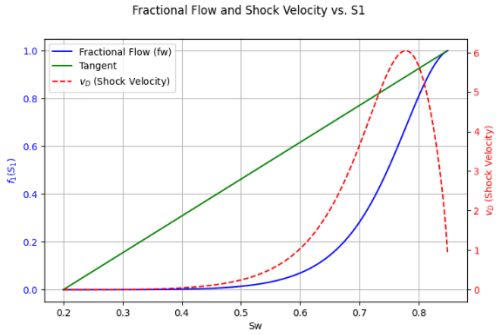

Figure 8. Fractional flow and shock velocity vs Sw for Case 3

For Case 3: The top-left plot presents two relative permeability curves, one for the wetting phase (water) and another for the non-wetting phase (CO_2). Since CO_2 is non-wetting, its relative permeability declines rapidly as water saturation increases. This indicates that at higher water saturations, CO_2 struggles to flow and can become trapped in the pore spaces. In contrast, water, as the wetting phase, maintains a higher effective permeability, allowing it to move more easily through the rock as saturation rises. Water readily channels through the pores, while CO_2 encounters fewer conductive pathways, leading to significant trapping of the non-wetting phase.

The top-right plot (Fractional Flow vs. Saturation and Shock Velocity) illustrates how water's proportion of the total flow changes with saturation and how quickly the saturation front moves. The fractional flow function increases gradually at low saturations but becomes steeper as water saturation rises. Physically, this means that once the pores are filled with water, nearly all flow is carried by water. Since water retains considerable relative permeability even as CO_2 saturation declines, the water front (shock) progresses steadily, displacing CO_2. Once water saturation surpasses a certain threshold, the non-wetting phase becomes largely immobile, effectively "locking in" the shock front.

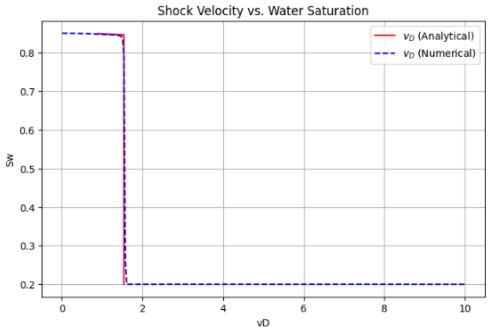

Figure 9. Comparison of numerical and analytical solution of Buckley Leverett for case 3

The numerical solution closely aligns with the analytical curve, confirming the finite difference method's accuracy. When the shock velocity is high, water saturation remains low—indicating that water (the wetting phase) is advancing quickly but with limited pore-space invasion. As velocity decreases, the shock front slows, allowing more water to occupy the pores and thus increasing the overall water saturation.

In this setup, water displaces CO_2, which is the non-wetting phase. Because water is the wetting fluid, it more easily invades smaller pores, trapping CO_2 in larger channels or behind the advancing front. This behavior reflects imbibition (wetting fluid entering a medium initially filled with non-wetting fluid), rather than drainage. The plot of Shock Velocity vs. Water Saturation illustrates this dynamic, showing how the shock velocity varies with changes in water saturation, further emphasizing the interplay between the wetting and non-wetting phases.

b. Spontaneous Imbibition:

The analytical solution in this code is derived by iteratively solving the fractional flow function F1(S) and the characteristic speed C^2, which are key to modeling two-phase fluid flow in porous media. Just likes what I have written on the methodology above, the key steps for analytical solution include: calculate the effective saturation, relative permeability, capillary pressure, capillary dispersion, initial guess, C^2 function, imbibition fractional flows, and omega.

The numerical solution uses finite differences to compute diffusion coefficients and numerical quadrature (quad) to iteratively solve the transport equation. For the grid lock size I used 0.01, the time step is 10, and the number of timesteps is 31536000 (for T = 1 year, with dt = 10 seconds)

- **Case 2:**

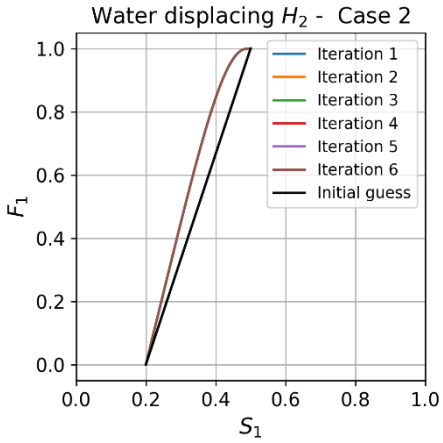

Figure 10. Capillary fractional flows for case 2

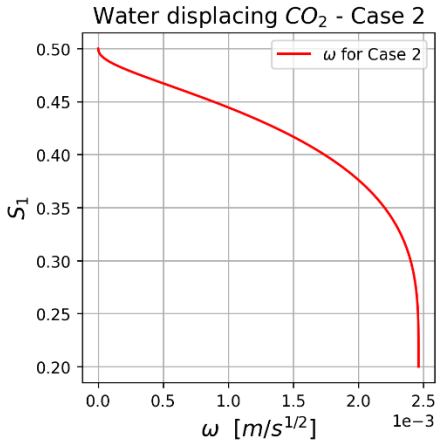

Figure 11. The omega plot from analytical solution for case 2

The left image shows rapid convergence from a linear guess to a smooth curve, indicating stable imbibition. The steep rise of F1 at low saturations reflects strong capillary forces efficiently displacing the non-wetting phase, confirming a water-wet system with full saturation at F1 = 1.

The right image depicts a sharp F1 decrease, suggesting high dispersion at higher saturations. As S1 decreases, capillary forces dominate, influencing the rate of change (ω). A high ω stabilizes at higher saturation, with a large area under its curve indicating strong capillary energy, reinforcing water-wet behavior.

The calculated C value is 6.83×10^{-5} m/√s, and the CCC value of 68.3 exceeds the strongly water-wet range. Combined with a viscosity ratio of 10.0, this confirms Case 2 as strongly water-wet, with high capillary dispersion and robust water imbibition.

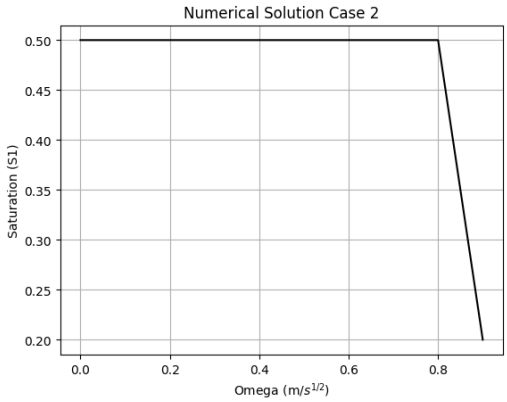

Figure 12. The omega plot from numerical solution for Case 2

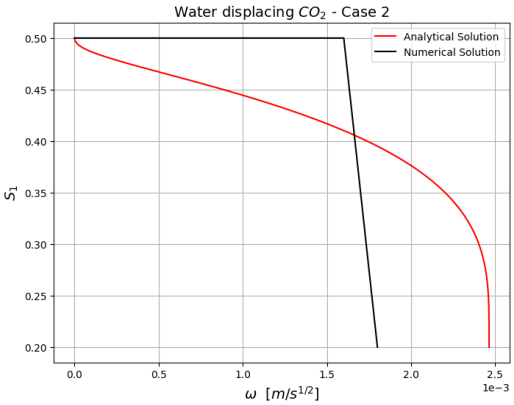

Figure 13. Comparison between analytical and numerical plot for Case 2

Numerical Solution Case 2: This plot shows the saturation profile obtained from the numerical solution. The x-axis represents the omega values (ω), and the y-axis represents the saturation ($S1$). The plot demonstrates how saturation changes with respect to omega, reflecting the numerical approximation of the fluid displacement process.

Water Displacing CO2 - Case 2: This plot compares the analytical and numerical solutions for the same scenario. The analytical solution (red line) is derived from theoretical equations, while the numerical solution (black line) is obtained through computational methods. The differences between the two lines highlight the impact of approximations and discretization in the numerical approach. The x-axis represents omega (ω), and the y-axis represents saturation ($S1$). The plot illustrates how well the numerical solution approximates the analytical solution, with discrepancies arising from factors like discretization errors and boundary condition handling.

- **Case 3:**

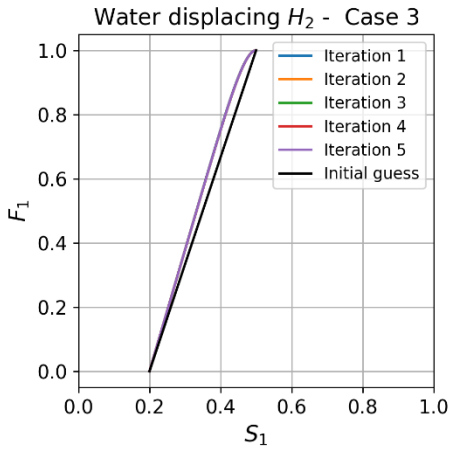

Figure 14. Capillary fractional flows for case 3

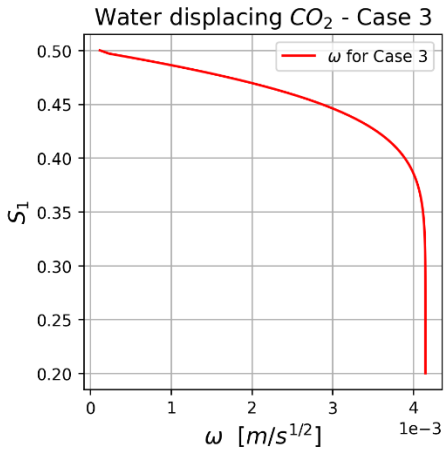

Figure 15. The omega vs water saturation plot for case 3

The left image shows rapid convergence from a linear guess to a smooth curve, indicating stable imbibition. The steep rise of F1 at low saturations reflects strong capillary forces efficiently displacing the non-wetting phase, confirming a water-wet system with full saturation at F1 = 1.

The right image depicts a sharp F1 decrease, suggesting high dispersion at higher saturations. As S1 decreases, capillary forces dominate, influencing the rate of change (ω). A high ω stabilizes at higher saturation, with a large area under its curve indicating strong capillary energy, reinforcing water-wet behavior. These trends align with the left image, highlighting the role of capillary forces in fluid displacement.

The calculated C value is 13.5×10^{-5} m/√s, slightly below the weakly water-wet range but above mixed-wet values. With a viscosity ratio of 4.0, Case 3 is classified as weakly water-wet, though close to mixed-wet behavior, influenced by viscosity and pore geometry.

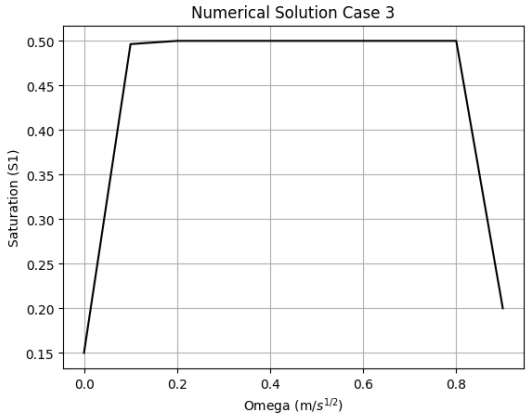

Figure 12. The omega plot from numerical solution for Case 3

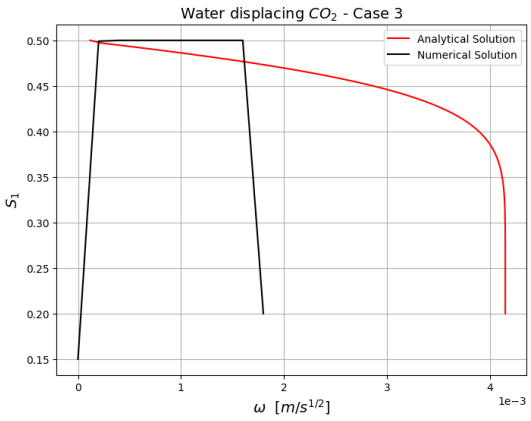

Figure 13. Comparison between analytical and numerical plot for Case 3

Numerical Solution Case 3: This plot displays the saturation profile from the numerical solution. The x-axis represents omega (ω), and the y-axis represents saturation ($S1$). It illustrates how saturation varies with omega, showcasing the numerical approximation of the fluid displacement process.

Water Displacing CO2 - Case 3: This plot compares the analytical and numerical solutions. The analytical solution (red line) is based on theoretical equations, while the numerical solution (black line) is derived computationally. The differences between the two lines emphasize the effects of approximations and discretization in the numerical method. The x-axis represents omega (ω), and the y-axis represents saturation ($S1$). The plot highlights the accuracy of the numerical solution relative to the analytical one, with discrepancies due to factors like discretization errors and boundary condition handling.

4. CONCLUSION

This study examines three different fluid displacement scenarios in porous media, focusing on how wetting and non-wetting phases interact based on relative permeability, fractional flow, and shock velocity.

- **Case 1 (CO_2 displacing water):** This is a drainage process where CO_2, being the non-wetting phase, flows more easily through larger pores, while water gets trapped in smaller ones due to capillary forces. The sharp rise in the fractional flow curve suggests a sudden displacement front. Numerical results confirm the accuracy of the finite difference method. Since water is being pushed out, imbibition is not relevant in this case.
- **Case 2 (Water displacing H_2):** Here, water—acting as the wetting phase—spreads into smaller pores and traps H_2 in the larger ones. The fractional flow curve shows a steady advance of the water front, and the numerical model aligns well with analytical predictions. This system is classified as strongly water-wet, with high capillary dispersion and strong water imbibition. The numerical solution for this case demonstrates how saturation changes with respect to omega, reflecting the numerical approximation of the fluid displacement process. The comparison between analytical and numerical solutions highlights the impact of approximations and discretization, with discrepancies arising from factors like discretization errors and boundary condition handling.

- **Case 3 (Water displacing CO_2):** Similar to Case 2, water moves into smaller pores while trapping CO_2 in larger spaces. The trends in shock velocity highlight how capillary forces control the displacement process. This system is considered weakly water-wet, leaning toward mixed-wet behavior due to the influence of viscosity and pore structure. The numerical solution for this case illustrates how saturation varies with omega, showcasing the numerical approximation of the fluid displacement process. The comparison between analytical and numerical solutions emphasizes the effects of approximations and discretization, with discrepancies due to factors like discretization errors and boundary condition handling.

In summary, the study underscores the importance of capillary forces and wetting characteristics in fluid movement through porous media, with numerical simulations closely matching theoretical expectations. The numerical solutions for Cases 2 and 3 demonstrate the effectiveness of computational methods in approximating analytical results, while also highlighting the inherent limitations due to discretization and boundary condition handling.

APPENDIX 1:

REFERENCES

Al-Hadhrami, H., Blunt, M. (2001). Thermally induced wettability alteration to improve oil recovery in fractured reservoirs. SPE Reservoir Eval. Eng. 4(03): 179-186

Anderson, W. (1986). Wettability literature part survey-part2 : wettability measurement. *J. Pet. Technol*, 38(11): 1246-1262

Arabzai, A. and Honma, S. (2013). Numerical simulation for Buckley-Leverett problem. *Proc. Schl. Eng. Tokai Univ., Ser. E.*, 38: 9-14

Morrow, N.R. and Masson, G. (2001). Recovery of oil by spontaneous imbibition. *Current Opinion Colloid & Interface Science*, 6(4): 321-337